



The SGLT2 Inhibitor Canagliflozin Reduces Atherosclerosis by Enhancing Macrophage Autophagy

Hongping Chen^{1,2} · Da Teng^{1,2} · Bowen Xu³ · Chunxiao Wang² · Hua Wang² · Wenjuan Jia² · Lei Gong² · Haibin Dong² · Lin Zhong² · Jun Yang²

Received: 28 September 2022 / Accepted: 23 January 2023 / Published online: 1 May 2023
© The Author(s), under exclusive licence to Springer Science+Business Media, LLC, part of Springer Nature 2023

Abstract

It has been shown that SGLT2 suppresses atherosclerosis (AS). Recent studies indicate that autophagy widely participates in atherogenesis. This study aimed to assess the effect of canagliflozin (CAN) on atherogenesis via autophagy. Macrophages and ApoE^{-/-} mice were used in this study. In macrophages, the results showed that CAN promoted LC3II expression and autophagosome formation. Furthermore, the cholesterol efflux assay demonstrated that CAN enhanced cholesterol efflux from macrophages via autophagy, resulting in lower lipid droplet concentrations in macrophages. The western blot revealed that CAN regulated autophagy via the AMPK/ULK1/Beclin1 signaling pathway. CAN resulted in increased macrophage autophagy in atherosclerotic plaques of ApoE^{-/-} mice, confirming that CAN could inhibit the progression of AS via promoting macrophage autophagy. The current study found that CAN reduced the production of atherosclerotic lesions, which adds to our understanding of how SGLT2 inhibitors function to delay the progression of AS.

Keywords SGLT2 inhibitor · Macrophage · Autophagy · Atherosclerosis

Abbreviations

CAD	Coronary artery disease
AS	Atherosclerosis
SGLT2	Sodium-Glucose Co-Transporter 2
ApoE	Apolipoprotein E
ApoE ^{-/-}	Apolipoprotein E deficient
HFD	High-fat diet
ox-LDL	Oxidized low-density lipoprotein
AMPK	Adenosine 5'-monophosphate-activated protein kinase

ULK1	UNC-51-like autophagy-activating kinase 1
ATG	Autophagy-related gene

Introduction

Coronary heart disease is a kind of chronic arterial atherosclerotic heart disease [1, 2], and it is a leading cause of death in both developed and developing nations [3]. Several risk factors, including smoking, obesity, abnormal blood glucose, dyslipidemia, hypertension, inflammatory response, etc., are associated with the pathogenesis of AS [4]. Prevention and treatment of AS have risen to the forefront of cardiovascular disease discourse.

Sodium-glucose cotransporter-2 (SGLT2) is largely expressed in the S1 and S2 segments of the proximal tubule of the kidney. This is the region of the kidney that is responsible for reabsorbing 90% of primary urine glucose [5]. Recently, SGLT-2 inhibitors have been developed as novel therapeutic agents for the treatment of patients with type 2 diabetes mellitus (T2DM). Multiple clinical trials have shown that SGLT2 inhibitors may give benefits beyond the treatment of diabetes, including a reduction in the risk of hospitalization for heart failure or death from cardiovascular causes. These benefits are now accessible to individuals with

Hongping Chen and Da Teng contributed equally to this work.

Associate Editor Guoping Li oversaw the review of this article.

✉ Lin Zhong
yizun1971@126.com

✉ Jun Yang
yangjyhd@163.com

¹ School of Medicine, Qingdao University, Qingdao, China

² Department of Cardiology, Yuhuangding Hospital, The Fourth School of Clinical Medicine of Qingdao University, Yantai, Shandong Province, China

³ Binzhou Medical University, Yantai, Shandong Province, China

and without T2DM [6, 7]. SGLT2 inhibitors may benefit the cardiovascular system by reducing adipose tissue-mediated inflammation and pro-inflammatory cytokine production, promoting ketone bodies as the metabolic substrate for the heart and kidneys, reducing oxidative stress, lowering serum uric acid levels, reducing glomerular hyperfiltration and albuminuria, and suppressing advanced glycation end-product signaling [8]. Xu et al. found that empagliflozin reduces obesity-induced inflammation and insulin resistance by promoting the conversion of white fat to brown, increasing fat metabolism, and activating M2 macrophage polarization, which may be an important pathway for the cardiovascular benefits of SGLT2 [9, 10].

Autophagy is a complex process inside cells that uses lysosomes to break down parts of the cytoplasm. It has been linked to metabolic diseases like AS [11, 12]. It is currently believed that autophagy is involved in the breakdown of lipid droplets (LDs), and autophagy-controlled cholesterol outflow from cells is a key part of keeping cholesterol levels stable [13]. Increased macrophage autophagy improves cholesterol efflux, lowers the cholesterol content of aortic AS plaques, which successfully maintains cholesterol balance and helps to prevent the onset and progression of AS [14]. Collectively, macrophage autophagy plays an important role in the pathogenesis of AS. Since therapeutic SGLT2 leads to substantial loss of energy in the form of glucose via sodium–glucose co-transporter, it is an intriguing possibility that SGLT-2 inhibitors may affect the level of cellular autophagy following the intracellular energy changes. The present study aimed to evaluate whether canagliflozin (CAN), a kind of SGLT2, can suppress the progression of AS by regulating macrophage autophagy.

Methods

Cell Culture and Experimental Design

The human monocyte (THP-1) was purchased from the American Type Culture Collection (ATCC). After resuscitation, the cells were cultured in 1640 medium (BI, Israel) containing 10% fetal bovine serum (FBS) (BI, Israel), 5% β -mercaptoethanol (sigma, USA), and 1% penicillin–streptomycin (MCE USA) at 37 °C with 5% CO₂. Then the cells at logarithmic growth phase were treated with phorbol 12-myristate-13-acetate (PMA) (Sigma, USA) for 24 h followed by ox-LDL (80 μ g/ml) (Yiyuan Biotechnologies, China) alone for 48 h to become atherosclerotic macrophages for further investigations [15]. In this work, rapamycin (MCE, USA) was used to induce autophagy, and 5 mM was found to be the optimal concentration. Like other cellular pathways, autophagy has a highly dynamic, multi-step process that includes the formation and destruction of

autolysosomes. To find out how CAN regulates autophagy, Bafilomycin A1 (BAF) (MCE, USA) was used in an in vitro study. BAF is a V-type ATPase inhibitor that prevents autophagosomes and lysosomes from forming autolysosomes via membrane potential regulation, thereby inhibiting autophagosome degradation [16]. The macrophages were grouped as follows: (1) the control group; (2) the CAN group (10 μ M); (3) the CAN + BAF (100 nM) group; and (4) the BAF (100 nM) group. For group (4), BAF was administered 2 h before harvesting.

Cell Viability Assay

Cell viability was measured using the Cell Counting Kit-8 (MCE, USA) according to the manufacturer's instructions.

Autophagic Flow Evaluation

Monomeric red fluorescent protein-green fluorescent protein-tagged LC3 adenoviral vectors (mRFP-GFP-LC3) were developed and synthesized by HANBIO (Shanghai, China). THP-1 cells were induced into macrophages on a 12-well plate, then transfected with mRFP-GFP-LC3 adenovirus and treated with ox-LDL for 48 h. After 12 h of CAN (10 μ M/L) intervention, the cell slides were subjected to the following treatments: The cells were fixed in 4% paraformaldehyde for 30 min in the dark, washed twice with PBS, and then penetrated for 10 min in the dark with 0.1% Triton. An anti-fluorescence quencher containing DAPI was used to quench the slides. Autophagic flow was observed using a confocal laser scanning microscope (Zeiss, Germany). Red/yellow puncta indicated autophagic flow.

Cell Lipid Assessment

THP-1 cells were transferred to slides in a 12-well plate and differentiated into macrophages with PMA as described above. Cells were classified into the following groups: (1) the control group; (2) the CAN group; and (3) the CAN + 3-methyladenine (3-MA) (1 mM) (MCE, USA) group. After 48 h of incubation with ox-LDL, the lipid content of cells was determined by Oil Red O staining. Photographs were taken using a microscope (Olympus, Japan) and quantified using Image J software (<https://imagej.nih.gov/ij/>, Version 1.53n, 7 November 2021). Oil Red area (%) = (positive area/all cells area) \times 100%.

Cholesterol Efflux Assay

The Cholesterol Efflux Assay Kit (Abcam, UK) was employed to detect cellular cholesterol efflux. Macrophages were cultivated with fluorescence-labeled cholesterol for 1 h, then equilibrated overnight. After 16 h, the cells were grown

in pre-treated human serum, which served as a cholesterol acceptor with the addition of 3-MA. After a 4-h co-incubation, supernatant and cell lysate were transferred to new 96-well plates. Supernatant and cell lysate absorbance were measured at 482/515 nm (BMG LABTECH, PHERAstar FSX, Germany). The formula for cholesterol efflux: Cholesterol efflux (%) = supernatant fluorescence intensity / (cell lysate fluorescence intensity + supernatant fluorescence intensity) 100%.

Animal Experiments

Eight-week-old female ApoE^{-/-} mice (C57BL/6 J Inv, Jackson Laboratory) were obtained from Nanjing GemPharmatech Company (Nanjing, China) and were fed a standard laboratory chow diet for 1 week. Following that, each animal was randomly assigned to one of three groups ($n = 15$ in each group): mock, high fatty diet (HFD), and HFD + CAN. Mock mice were fed a regular diet, whereas the HFD and HFD + CAN groups were provided a high-fat diet for 12 weeks. At the same time, the HFD + CAN mice were fed CAN (10 mg/kg/day) by gavage, and the mock and HFD mice were fed the same volume of 0.5% hydroxypropyl methylcellulose/day. All tests were conducted in accordance with the American Heart Association's recommendation for the design, execution, and reporting of animal atherosclerosis studies [17]. All mice were weighed weekly. Anesthetized 21-week-old mice were bled retro-orbitally and their hearts were preserved in 4% paraformaldehyde (Sigma, USA) and paraffin embedded. The serum was isolated from the blood sample by centrifugation for 15 min at 3000 rpm. The aortic tissues were snap-frozen in liquid nitrogen. All tissues were kept at -80°C . All institutional and national guidelines for the care and use of laboratory animals were followed and approved by the appropriate institutional committees.

Western Blot Analysis

Proteins were extracted from treated macrophages and ApoE^{-/-} mice aortas. All samples were lysed in RIPA buffer for 30 min (Beyotime, China). Proteins on gels were transferred to 0.22 m PVDF membranes (Millipore, Germany). Then the PVDF membranes were incubated with primary antibodies overnight at 4°C after being blocked with 5% skimmed milk (Spark jade, China) or 3% bovine serum albumin (Yeasen Biotech, China) for 1 h at room temperature. All primary antibodies are shown in the supplemental materials. After an hour with horseradish peroxidase-labeled secondary antibodies and washing $3 \times$ with TBST, bands were detected by ECL chemiluminescence (Vazyme, China).

Immunofluorescence Staining

The aorta tissues were dehydrated in 30% sucrose after 48 h in 4% paraformaldehyde. After, the tissues were permeabilized for 20 min at room temperature with 0.1% Triton X-100 (Solarbio, China) before being embedded with OCT (SAKURA, Japan). The slices were blocked for 30 min in 5% goat serum before being treated with the primary antibody overnight at 4°C . After three PBS washes, the slices were incubated with the secondary antibody for 1 h at room temperature, followed by being treated with DAPI for the nuclei. Images captured with a fluorescence microscope were measured using Image J software (Leica Microsystems, Mannheim). LC3 and CD68 were the primary antibodies used (Abcam, UK). LC3 and CD68 in plaque (%) = (staining positive/plaque) 100%.

Hematoxylin and Eosin Staining

HE staining was applied to measure the plaque level. Concisely, after dewaxing, the slices were stained for 30 s with hematoxylin and blued for 5 min with alkaline water. The slices were then dyed with eosin for 1 min and washed with double distilled water (DDW). Leica Microsystems (Mannheim, Germany) microscope images were quantified with Image J software. Plaque area (%) = (plaque area / aortic root area) \times 100%.

Oil Red O Staining

Oil Red O staining was taken to measure the lipid content in plaque. After washing $3 \times$ with PBS, the frozen slices were fixed in 4% paraformaldehyde for 20 min, followed by being incubated at 37°C for 30 min with Oil Red O solution (Solarbio, China). The slices were photographed under a microscope (Olympus, Japan) after 75% ethanol washing for 3 s. The aortic tissues were stained using the same method. Oil Red area (%) = (staining positive area / plaque area) \times 100%.

Masson Staining

The collagen in the plaque was evaluated with the method of Masson staining (Sigma, USA). In short, the nuclei were stained black with Weigert's iron hematoxylin, the cytoplasm and muscle fibers were stained red with Biebrich scarlet-acid fuchsin, and collagen was stained blue with aniline blue following treatment with phosphotungstic and phosphomolybdic acid. Photographs were taken with a microscope (Olympus, Japan) and quantified using Image J software. Collagen area (%) = (staining positive area / plaque area) \times 100%.

Transmission Electron Microscopy

Anesthetized mice were perfused with frozen 0.9% normal saline (NS) for 5 min, followed by 10 ml of frozen 4% paraformaldehyde. Dissected aorta samples were fixed in 3% glutaraldehyde for 2 h at 4 °C. Aortic tissues were then rinsed in 0.1 M PBS 3× before being fixed with 1% osmium tetroxide at 4 °C for 90 min. Following overnight incubation at 35 °C, tissues were embedded in Epon 812 mix after dehydration in graded ethanol. Finally, the tissues were heated at 37 °C for 12 h, 45 °C for 12 h, and 60 °C for 24 h. The MT-X ultramicrotome produced ultrathin slices (70 nm) on 100 mesh copper grids. After 15 min of staining with 2% uranyl acetate and 5 min of staining with lead citrate, the slices were viewed with a 120 kV transmission electron microscope (TEM) (Technai G2 Spirit Twin device).

Statistical Analysis

Statistical analyzes were performed using GraphPad PRISM 8.0 software (GraphPad Software, La Jolla, USA). Unless otherwise noted, data is presented as means ± SDs (error bars). The Shapiro–Wilk test was used to determine the normality of the data, and the Brown-Forsythe test was used to determine the equality of group variance. Student *t* tests (2-tailed unpaired) were used to compare two groups, and a one-way ANOVA followed by a Bonferroni post hoc test was used to compare more than two groups. Nonparametric data were analyzed using the Mann–Whitney *U* test or the Wilcoxon matched-pairs signed-rank test, respectively. Differences with a *P* value < 0.05 were considered significant.

Results

CAN Promoted Autophagy in Macrophages During the Autophagic Vesicle Formation Phase

As an inhibitor of glucose sodium translocase, CAN may affect cellular activity. The CCK8 assay was employed to check cellular vitality, and the results indicated a gradual decrease in cell viability with increasing drug concentrations when macrophages were co-cultured with CAN (Fig. 1a). In this work 10 μM of CAN was found to be the optimal concentration. To determine the optimal period for CAN intervention on macrophages, we established three time points at 12, 24, and 48 h. At 12 h, the expression of Beclin-1 and LC3II was considerably higher and p62 lower in the CAN group than in the control group, but at 24 and 48 h, there was no statistical difference between the two groups. (Fig. 1b–e).

To further explore how CAN regulated macrophage autophagy, BAF was used in the in vitro study. The western blot revealed that LC3II was significantly higher in the

CAN group than the control group but significantly lower than the BAF and CAN + BAF groups. In comparison to the FCAN + BAF group, meanwhile, LC3II was significantly lower in the BAF group (Fig. 1f and g). To investigate the effect of CAN on autophagy in macrophages more intuitively, the mRFP-GFP-LC3 adenovirus mentioned above was used to transfect and intervene macrophages for 48 h. As can be seen, there was a significant difference in autophagosomes among the experimental groups, which was consistent with western blot (Fig. 1h and i). The results above demonstrated that CAN promoted autophagy during the autophagosome formation stage.

CAN Promoted Macrophage Autophagy Through AMPK/ULK1/Beclin1 Signaling Pathway

As an agent that affects glucose transport, CAN is anticipated to modulate the activation of macrophage energy-related pathways. Previous studies have indicated that AMPK is affected by intracellular energy metabolism and regulates cellular autophagy [17]. As determined by western blot (Fig. 2a and e), unsurprisingly, CAN promoted the expression of phosphorylated AMPK protein. Then, we searched for AMPK's downstream pathway proteins. Intracellular signaling pathways that initiate autophagy are activated in response to a variety of intracellular stressors and nutritional status changes. These pathways are aimed at the UNC-like autophagy-activating kinase 1 initiation complex (ULK1) [9]. Western blot showed that CAN resulted in a significant increase in the expression of ULK1 phosphorylation (Fig. 2a and f). Finally, we investigated Beclin1, an important protein for autophagy, and discovered that it was significantly higher in the CAN group (Fig. 2a and b). However, the phosphorylation of AMPK, ULK1, and Beclin1 was neutralized by the addition of FTY720 (an AMPK inhibitor) in macrophages (Fig. 2h–m). In addition, the autophagosomes in the CAN + FTY720 group were significantly lower than those in the CAN group, which was consistent with western blot (Fig. 2n and o). This verified that CAN promoted autophagy by upregulating and activating the AMPK/ULK1/Beclin1 axis.

CAN Induced Lipid Droplet Translocation in Macrophage Via Autophagy

Recent investigations have demonstrated that autophagy increases the extracellular transfer of LDs in macrophages [18, 19]. To investigate if CAN modulates the extracellular transport of LDs via autophagy, the lipid content of macrophages was evaluated using Oil Red O staining. We observed that CAN decreased the number of LDs in macrophages, indicating that CAN was capable of reducing the LDs in macrophages. Then, 3-MA (an inhibitor of

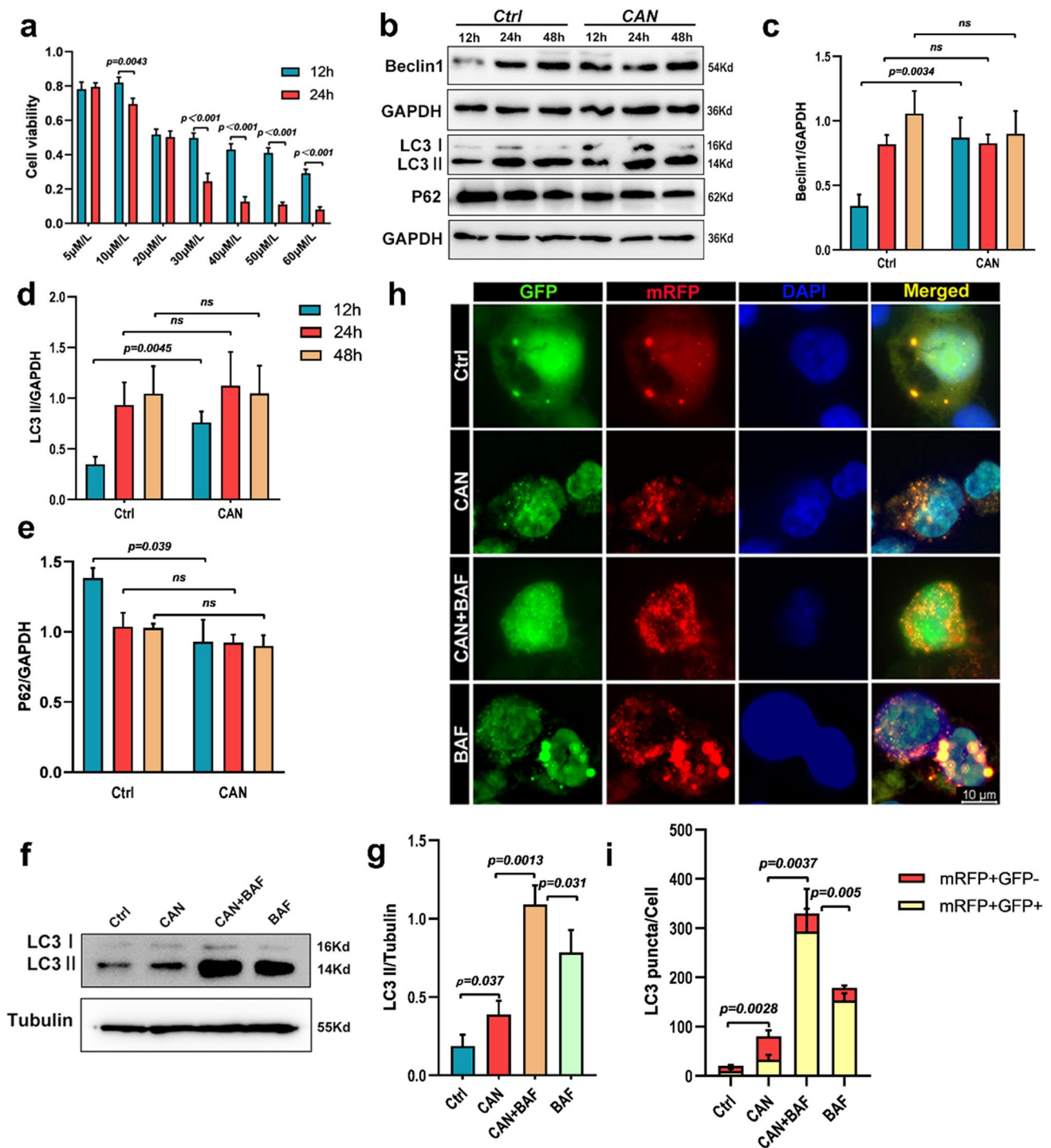


Fig. 1 CAN promoted autophagy in macrophages during the autophagic vesicle formation phase. **a** CCK8 assay of CAN and 10 μM of CAN was found to be the optimal concentration. **b–e** Representative western blots and relative quantitative analysis of LC3II, P62, and Beclin1 in macrophages treated with CAN. **f, g** Representative western blots and relative quantitative analysis of LC3II in mac-

rophages treated with CAN (10 μM), CAN+BAF (100 nM), and BAF (100 nM). **h, i** Representative images of the autophagosomes in macrophages after transfection of mGFP-RFP-LC3 adenovirus for 48 h. The experiment was repeated three times independently. Data were expressed as the means ± SDs. Scale bar: 10 μm. $P < 0.05$, $P < 0.01$, ns > 0.05 as determined by Student *t* test

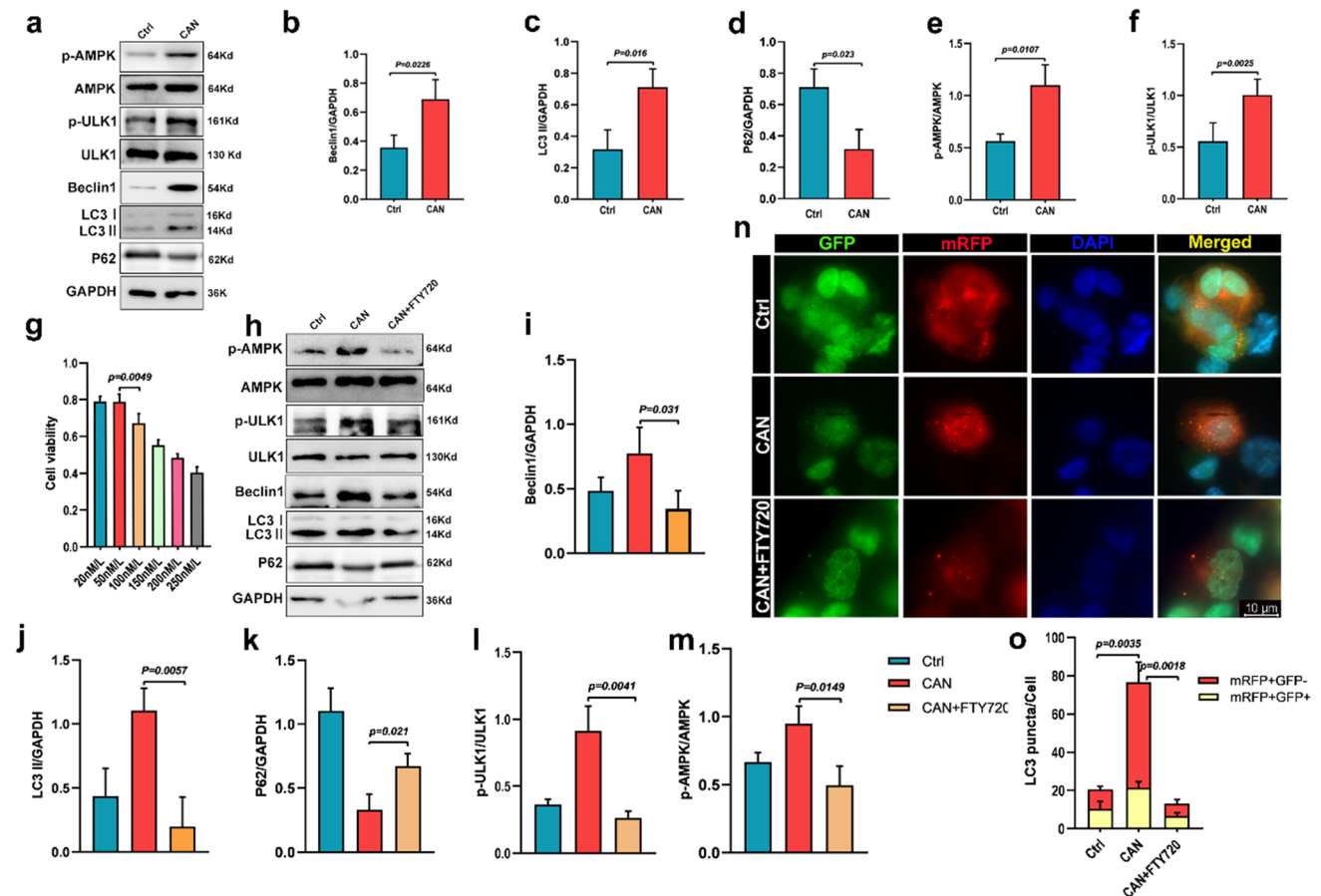


Fig. 2 CAN promoted macrophage autophagy through AMPK/ULK1/Beclin1 signaling pathway. **a–f** Representative western blots and relative quantitative analysis of the autophagic proteins in macrophages. **g** CCK8 assay of FTY720 (An AMPK inhibitor) and 50 nM of FTY720 was found to be the optimal concentration. **h–m** Representative western blots and relative quantitative analysis of

the autophagic proteins in macrophages with FTY720 (50 nM). **n, o** Representative images of the autophagosomes in macrophages with FTY720 (50 nM). The experiment was repeated three times independently. Data were expressed as the means \pm SDs. Scale bar: 10 μ m. $P < 0.05$, $P < 0.01$ as determined by Student's *t* test

autophagosome synthesis) was added to the culture of macrophages, and the results demonstrated that LDs in macrophages were dramatically elevated compared to the CAN alone (Fig. 3a and b). In addition, the cholesterol efflux assay demonstrated that CAN enhanced cholesterol efflux from macrophages via autophagy (Fig. 3c). Our data revealed that CAN induced autophagy and enhanced LDs extracellular transport in macrophages.

CAN Inhibited Atherosclerotic Lesion Formation and Promoted Plaque Stability in Mice

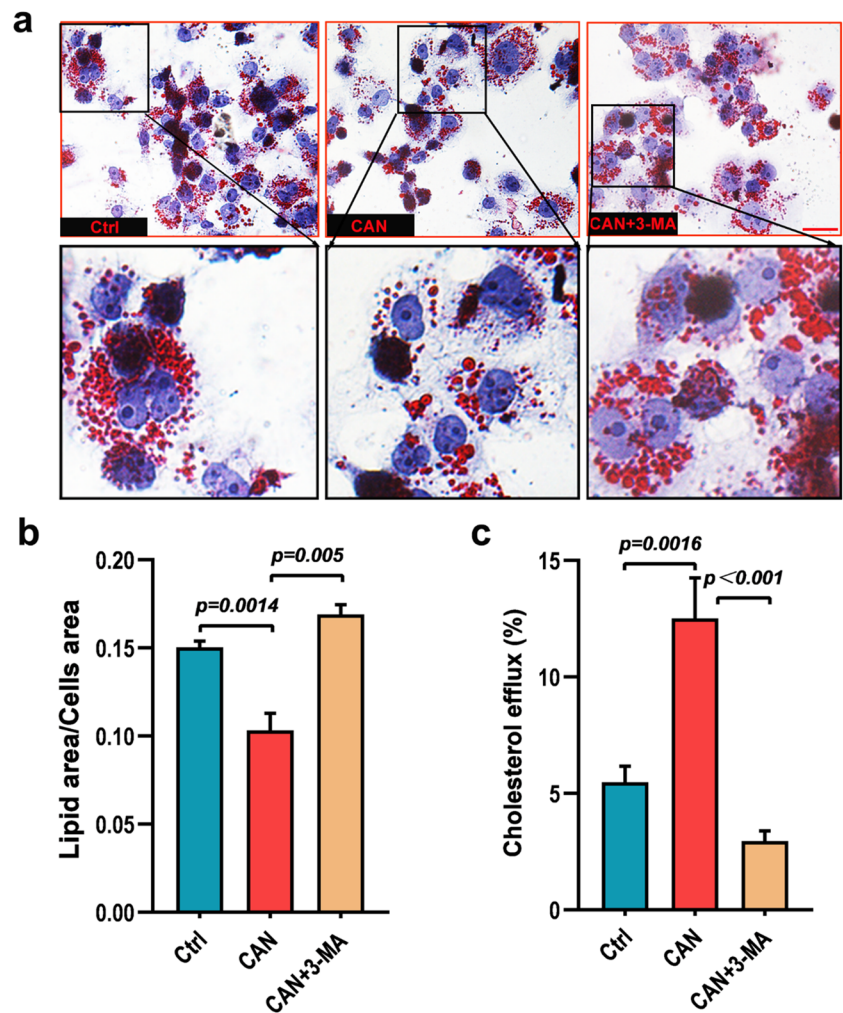
To determine whether CAN can prevent atherogenesis and to investigate potential mechanisms, eight-week-old ApoE $^{-/-}$ female mice were fed with CAN. Interestingly, CAN was found to significantly prevent the growth of intra-aortic plaques, which appears to be consistent with the *in vitro* outcomes (Fig. 4A–E). Rupture of atherosclerotic plaque due

to poor plaque stability is the main cause of cardiovascular events in clinical practice [20]. CAN slowed the progression of atherosclerotic lesions, but its effect on plaque stability needed to be determined. The Shiomi plaque vulnerability index is commonly used to evaluate plaque stability [21]. In the present work, CAN decreased the number of macrophages and lipids but increased the number of smooth muscle cells and collagen in the atherosclerotic plaques of ApoE $^{-/-}$ mice, hence contributing to plaque stability (Fig. 4F–K). Taken together, these findings suggested that CAN prevented atherosclerotic lesion formation and promoted plaque stability *in vivo*.

CAN Enhanced Macrophage Autophagy in ApoE $^{-/-}$ Mice Atherosclerotic Plaques

To determine if CAN enhanced autophagy upregulation in macrophages, we assessed the expression of LC3II and P62 in plaques via western blot. Compared with the HFD group,

Fig. 3 CAN induced lipid droplet translocation in macrophage via autophagy. **a**, **b** Representative photomicrographs and analysis of lipid droplets in macrophage after Oil red O staining ($\times 10$, $\times 40$). **c** Cholesterol efflux assay in macrophages treated with CAN and CAN + 3-MA (1 mM). Data were expressed as the means \pm SDs. Scale bar: 100 μ m ($\times 10$). $P < 0.05$, $P < 0.001$ as determined by Student's *t* test



LC3II expression was sharply increased in the HFD + CAN group, while P62 was decreased. Likewise, immunofluorescence revealed that CAN stimulates the synthesis of LC3II (Fig. 5a–e). To further visualize autophagy, we calculated the number of autophagic vesicles within macrophages within plaques using TEM. We observed that CAN stimulated autophagosome formation in macrophages (Fig. 5f and g). As with in vitro research, the foregoing results demonstrated that CAN increase autophagy within plaque macrophages.

Discussion

One of the most prevalent complications of diabetes is atherosclerosis [22]. In the treatment of diabetes, SGLT2 inhibitors have risen to the position of being the hypoglycemic medicines of first-line treatment. There is more and more evidence that SGLT2 inhibitors help control lipid

metabolism and slow the progression of atherosclerosis [23–26]. The purpose of this study was to explore the role of SGLT2 inhibitors in the progression of AS and to try to reveal new mechanisms of the action. In the present work, we discovered that CAN prevented atherosclerotic plaque development via increasing macrophage autophagy.

Intracellular glucose metabolism plays a pivotal role in the activation of autophagy [27]. SGLT2 is a member of the sodium glucose cotransporter family, which are sodium-dependent glucose transport proteins. SGLT2 inhibitors down-regulate cellular glucose transport, which may lead to a relative lack of energy in macrophages and thus promote the production of intracellular autophagy. Unsurprisingly, we discovered that CAN stimulated autophagy in macrophages (Fig. 1b and d). The complicated intracellular physiological process of autophagy involves the creation and destruction of autophagic vesicles [11]. In this investigation, we blocked the breakdown

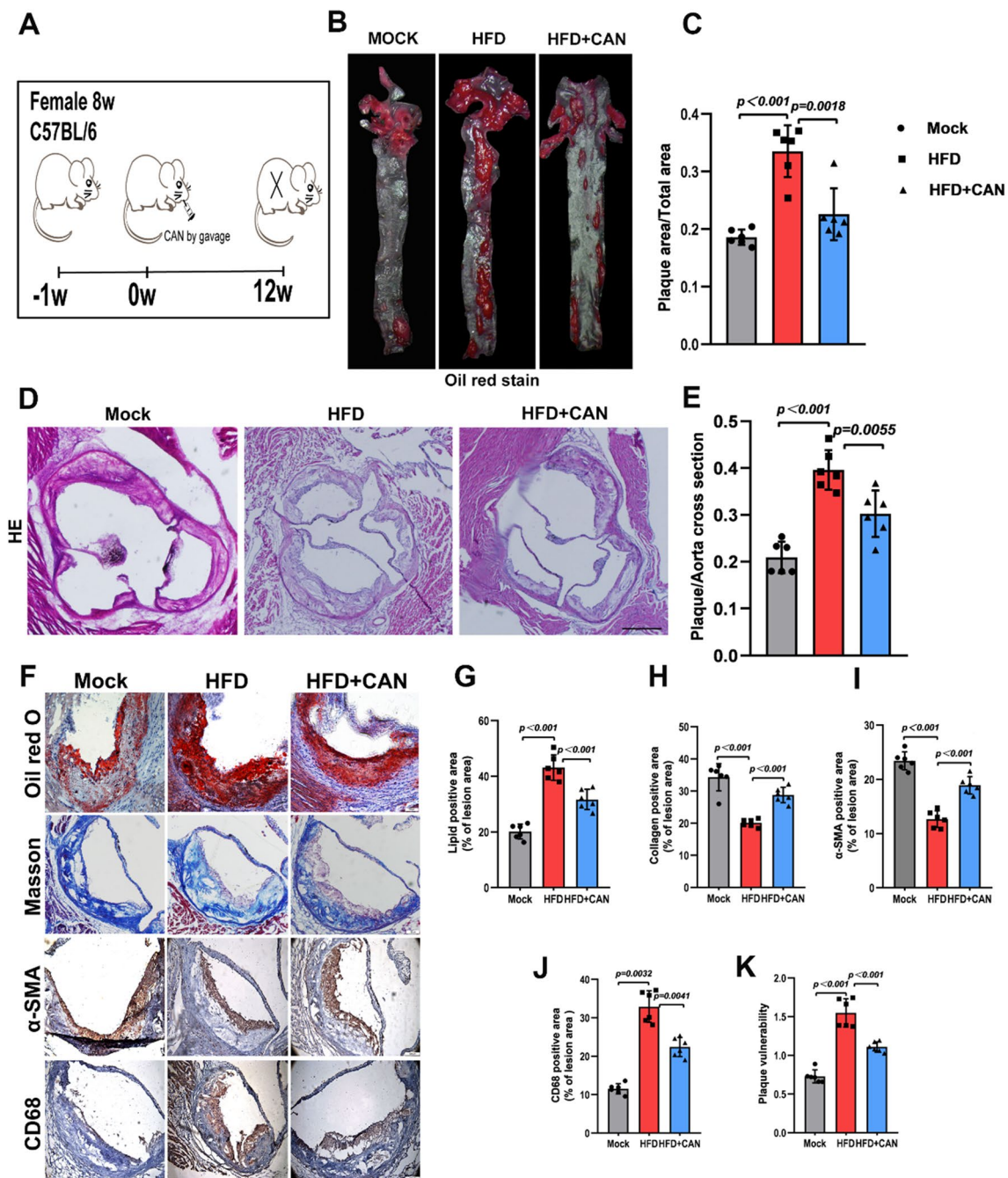


Fig. 4 CAN inhibited atherosclerotic lesion formation and promoted plaque stability in mice. **A** Schematic diagram of the experimental system. **B, C** Representative images and quantitative analysis of aorta en face stained with Oil red O and statistics of plaque area of whole aorta ($n=6$ /group). **D, E** Representative images quantitative analysis of aortic root atherosclerotic lesion stained with HE staining and quantification of aortic root lesion size ($n=6$ /group). **F–J** Representa-

tive images quantification of lipid, collagen, smooth muscle cells, and macrophages in plaques after staining ($\times 4, \times 10$) ($n=6$ /group). **K** Plaque vulnerability index [(Oil red O area + CD68 area)/(α -SMA area + collagen area)] in atherosclerotic plaque. Data were expressed as the means \pm SDs. Scale bar: 100 μ m ($\times 10$). $P < 0.05$, $P < 0.001$ as determined by Student's *t* test

of autophagic vesicles using BAF and observed that LC3II was considerably higher in the CAN + BAF group than in the BAF group, indicating that CAN enhances autophagy during the autophagosome formation phase (Fig. 1f–i).

AMPK is a crucial metabolic regulator that suppresses energy-consuming pathways and activates the compensated energy-producing pathways [27]. Glucose insufficiency activates AMPK, which in turn causes autophagy

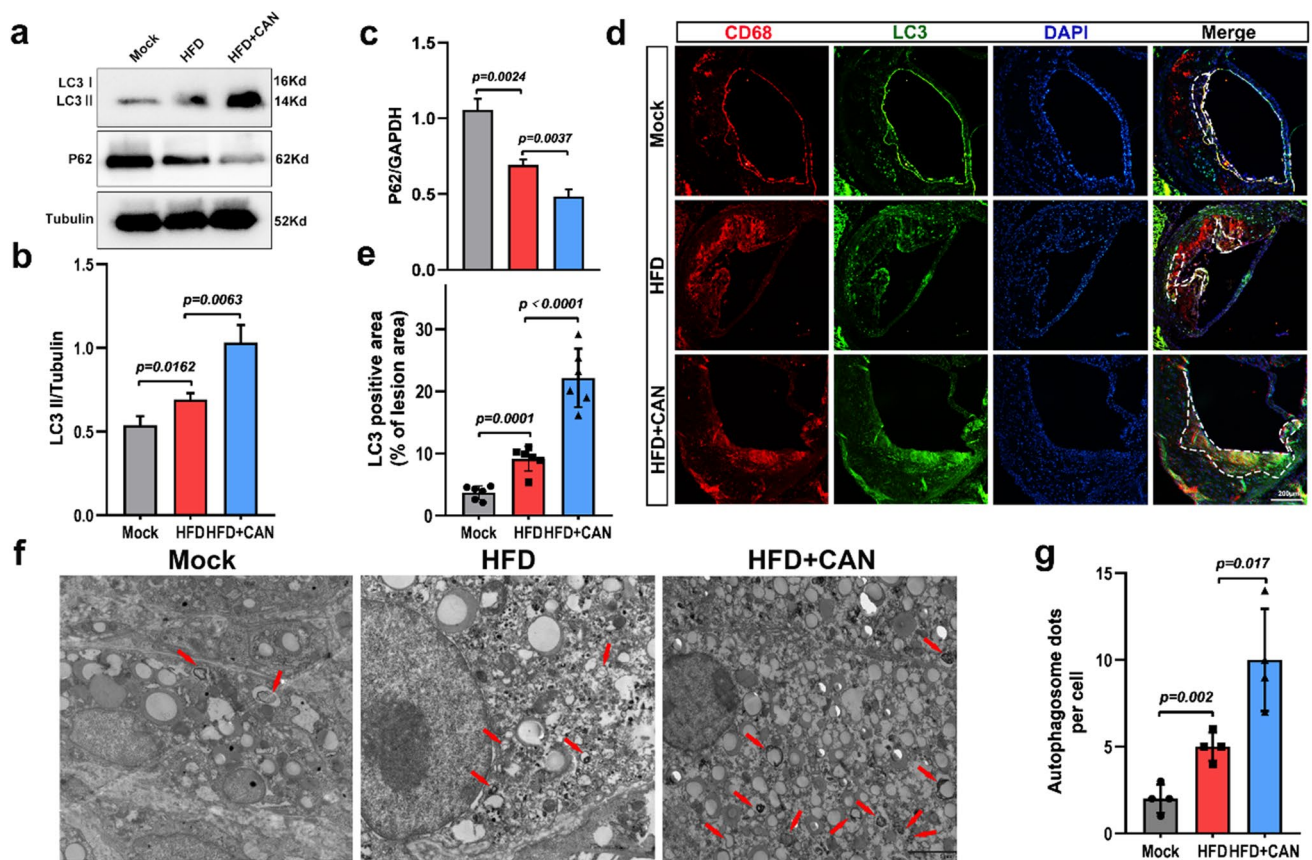


Fig. 5 CAN enhanced macrophage autophagy in ApoE^{-/-} mice atherosclerotic plaques. **a–c** Representative western blots and relative quantitative analysis of LC3II and P62 in three groups. The experiment was repeated three times independently. **d, e** Representative IF staining images and quantitative analysis of LC3 and CD68 immuno-

fluorescence co-localization in three groups ($n=6$ /group). Scale bar: 200 μ m. **f, g** Representative TEM images and quantitative analysis of autophagosomes in macrophages of plaques ($n=4$ /group). Scale bar: 5 μ m. Data were expressed as the mean \pm SDs. $P < 0.05$, $P < 0.01$ vs control as determined by Student's t test

[28, 29]. In this investigation, CAN dramatically stimulated AMPK activity (Fig. 2a and e), which was consistent with previous research [30]. Located downstream of AMPK, ULK1 is a crucial autophagy pathway protein [11]. The activation of the ULK1 complex initiates autophagy, which in turn activates a class III PI3K complex composed of the core components Beclin-1, VPS34/PIK3C3, and additional recruited variable components, with various class III PI3K complexes performing different functions. Then the Atg5-Atg12 complex, which is coupled to Atg16, promotes autophagosomal membrane expansion [31]. In this study, CAN significantly promoted the expression of phosphorylated ULK1 and Beclin1 (Fig. 2a, b, and f). Furthermore, we used the AMPK inhibitor FTY720 and found that the effects of CAN were attenuated (Fig. 2h–o). These results demonstrated that CAN may enhance autophagy by activating and upregulating the AMPK/ULK1/Beclin1 axis.

Autophagy has been known to improve macrophage lipid transport [13, 14]. In this experiment, CAN was observed

to increase the efflux of LDs from macrophages, and an autophagy inhibitor was able to attenuate this effect, indicating that CAN increases lipid efflux by enhancing macrophage autophagy (Fig. 3). It may explain, at least in part, why SGLT2 improves cardiovascular disease outcomes, including hospitalization for heart failure, death, and CVD, compared to other hypoglycemic medications.

Plaque instability is essential for cardiovascular events caused by atherosclerosis. According to our observations, CAN could improve the stability of atherosclerotic plaque. CAN increased the stability of atherosclerotic plaques, which is consistent with previous studies [32]. Several recent studies have revealed that SGLT2 inhibitors lower the volume of atherosclerotic plaques in mice and influence the composition of macrophages, collagen fibers, lipids, and smooth muscle cells [25, 33–36]. Interestingly, our study observed that increased CAN decreased macrophage infiltration in plaques (Fig. 4F and J). Reduced macrophages improved plaque stability [37]. In addition, we observed that CAN decreased LDs content in plaques, increased smooth

muscle cell numbers, and collagen production (Fig. 4F, J, I, and H), all of which could increase plaque stability.

Our study is limited in the following ways: to start, autophagy's role differs depending on the stage of atherosclerosis formation. The animals used in this study were treated for 21 weeks, and we should have used longer durations to better understand CAN's role in plaque autophagy. Second, in addition to macrophages, plaques contain smooth muscle cells and endothelial cells, and the control of autophagy by CAN in these two types of cells requires urgent investigation in order to fully assess CAN's regulatory effect on autophagy in plaques. Finally, we neglected to explore whether the effects of CAN on macrophages are modulated by hyperglycemia or insulin resistance, and we will explore this aspect in future studies. Besides, there are also some other drawbacks in this study: we used the THP-1 cell line for the pathway study, when in fact it would be better to isolate monocytes from human blood and induce their differentiation into macrophages with macrophage colony-stimulating factor (M-CSF). We did not knock down SGLT2 in *in vitro* experiments, which is the upstream regulator of the AMPK/ULK1/Beclin1 signaling pathway via CAN.

Conclusion

In the current study, it was revealed that CAN prevented the advancement of atherosclerotic plaques by activating macrophage autophagy and regulating macrophage lipid metabolism during the autophagosome formation phase via the AMPK/mTOR/Beclin1 axis. These findings expand our knowledge of how SGLT2 inhibitors function to prevent the progression of AS and introduce novel therapeutic approaches for the treatment of atherosclerotic diseases.

Supplementary Information The online version contains supplementary material available at <https://doi.org/10.1007/s12265-023-10390-w>.

Acknowledgements We thank Jiahui Wang, Peng Zhu, and Huishan Zhao (Central Laboratory, The Affiliated Yantai Yuhuangding Hospital of Qingdao University) for their technical assistance.

Funding Key Research and Development Program of Shandong Province (No. 2019GSF108142), Natural Science Foundation of Shandong Province (No. ZR2022MH151), National Natural Science Foundation of China (No. 81900310) (No. 82200503), Science and Technology Program of Yantai City (No. 2021MSGY042 and), Science and Technology Program of Yantai City (No. 2021MSGY044), and Youth Research Foundation of Yuhuangding Hospital (No. 2021–03).

All procedures followed were in accordance with the ethical standards of the responsible committee on human experimentation and with the Helsinki Declaration. Informed consent was obtained from all patients before being included in the study. The human research protocol was approved by the medical ethics committee of Yantai Yuhuangding Hospital, affiliated with Qingdao University (NO.2021–346). All Institutional and National Guidelines for the care and use of animals (fisheries) were followed. The animal research was approved by the Institutional Animal Care and Use Committee at Qingdao University (NO.QDU-AEC-2021176).

Data Availability The data that support the findings of this study are available on request from the corresponding author. The data are not publicly available due to privacy or ethical restrictions.

Declarations

Ethical Approval All procedures followed were in accordance with the ethical standards of the responsible committee on human experimentation and with the Helsinki Declaration. Informed consent was obtained from all patients before being included in the study. The human research protocol was approved by the medical ethics committee of Yantai Yuhuangding Hospital, affiliated with Qingdao University (NO.2021-346). All Institutional and National Guidelines for the care and use of animals (fisheries) were followed. The animal research was approved by the Institutional Animal Care and Use Committee at Qingdao University (NO.QDU-AEC-2021176).

Conflict of Interest The authors declare no competing interests.

References

- Moore KJ, Tabas I. Macrophages in the pathogenesis of atherosclerosis. *Cell*. 2011;145(3):341–55.
- Ross R. Atherosclerosis—an inflammatory disease. *N Engl J Med*. 1999;340(2):115–26.
- Global, regional, and national age-sex specific all-cause and cause-specific mortality for 240 causes of death, 1990–2013: a systematic analysis for the Global Burden of Disease Study 2013. *Lancet*. 2015. 385(9963): 117–71.
- Cervelli T, Borghini A, Galli A, Andreassi MG. DNA damage and repair in atherosclerosis: current insights and future perspectives. *Int J Mol Sci*. 2012;13(12):16929–44.
- Rieg T, Masuda T, Gerasimova M, et al. Increase in SGLT1-mediated transport explains renal glucose reabsorption during genetic and pharmacological SGLT2 inhibition in euglycemia. *Am J Physiol Renal Physiol*. 2014;306(2):F188–93.
- Kang A, Jardine MJ. SGLT2 inhibitors may offer benefit beyond diabetes. *Nat Rev Nephrol*. 2021;17(2):83–4.
- Khunti K. SGLT2 inhibitors in people with and without T2DM. *Nat Rev Endocrinol*. 2021;17(2):75–6.
- Cowie MR, Fisher M. SGLT2 inhibitors: mechanisms of cardiovascular benefit beyond glycaemic control. *Nat Rev Cardiol*. 2020;17(12):761–72.
- Xu L, Nagata N, Nagashimada M, et al. SGLT2 inhibition by empagliflozin promotes fat utilization and browning and attenuates inflammation and insulin resistance by polarizing M2 macrophages in diet-induced obese mice. *EBioMedicine*. 2017;20:137–49.
- Xu L, Ota T. Emerging roles of SGLT2 inhibitors in obesity and insulin resistance: focus on fat browning and macrophage polarization. *Adipocyte*. 2018;7(2):121–8.
- Kitava M, Koya D. Autophagy in metabolic disease and ageing. *Nat Rev Endocrinol*. 2021;17(11):647–61.
- Liao X, Sluimer JC, Wang Y, et al. Macrophage autophagy plays a protective role in advanced atherosclerosis. *Cell Metab*. 2012;15(4):545–53.
- Jeong SJ, Lee MN, Oh GT. The role of macrophage lipophagy in reverse cholesterol transport. *Endocrinol Metab (Seoul)*. 2017;32(1):41–6.
- Martinet W, De Meyer I, Verheye S, Schrijvers DM, Timmermans JP, De Meyer GR. Drug-induced macrophage autophagy in atherosclerosis: for better or worse. *Basic Res Cardiol*. 2013;108(1):321.

15. Stawowy P, Meyborg H, Stibenz D, et al. Furin-like proprotein convertases are central regulators of the membrane type matrix metalloproteinase-pro-matrix metalloproteinase-2 proteolytic cascade in atherosclerosis. *Circulation*. 2005;111(21):2820–7.
16. Klionsky DJ, Elazar Z, Seglen PO, Rubinsztein DC. Does bafilomycin A1 block the fusion of autophagosomes with lysosomes. *Autophagy*. 2008;4(7):849–50.
17. Daugherty A, Tall AR, Daemen M, et al. Recommendation on design, execution, and reporting of animal atherosclerosis studies: a scientific statement from the American Heart Association. *Circ Res*. 2017;121(6):e53–79.
18. He J, Zhang G, Pang Q, et al. SIRT6 reduces macrophage foam cell formation by inducing autophagy and cholesterol efflux under ox-LDL condition. *FEBS J*. 2017;284(9):1324–37.
19. Ouimet M, Franklin V, Mak E, Liao X, Tabas I, Marcel YL. Autophagy regulates cholesterol efflux from macrophage foam cells via lysosomal acid lipase. *Cell Metab*. 2011;13(6):655–67.
20. Hong MK, Mintz GS, Lee CW, et al. Comparison of coronary plaque rupture between stable angina and acute myocardial infarction: a three-vessel intravascular ultrasound study in 235 patients. *Circulation*. 2004;110(8):928–33.
21. Shiomi M, Ito T, Hirouchi Y, Enomoto M. Fibromuscular cap composition is important for the stability of established atherosclerotic plaques in mature WHHL rabbits treated with statins. *Atherosclerosis*. 2001;157(1):75–84.
22. Tomic D, Shaw JE, Magliano DJ. The burden and risks of emerging complications of diabetes mellitus. *Nat Rev Endocrinol*. 2022 : 1–15.
23. Pennig J, Scherrer P, Gissler MC, et al. Glucose lowering by SGLT2-inhibitor empagliflozin accelerates atherosclerosis regression in hyperglycemic STZ-diabetic mice. *Sci Rep*. 2019;9(1):17937.
24. Lauritsen KM, Voigt JH, Pedersen SB, et al. Effects of SGLT2 inhibition on lipid transport in adipose tissue in type 2 diabetes. *Endocr Connect*. 2022. 11(4).
25. Han JH, Oh TJ, Lee G, et al. The beneficial effects of empagliflozin, an SGLT2 inhibitor, on atherosclerosis in ApoE (-/-) mice fed a western diet. *Diabetologia*. 2017;60(2):364–76.
26. Xu J, Hirai T, Koya D, Kitada M. Effects of SGLT2 inhibitors on atherosclerosis: lessons from cardiovascular clinical outcomes in type 2 diabetic patients and basic researches. *J Clin Med*. 2021. 11(1).
27. Ha J, Guan KL, Kim J. AMPK and autophagy in glucose/glycogen metabolism. *Mol Aspects Med*. 2015;46:46–62.
28. Lin SC, Hardie DG. AMPK: Sensing glucose as well as cellular energy status. *Cell Metab*. 2018;27(2):299–313.
29. Wei L, Chen W, Zou Y, et al. AMP-activated protein kinase regulates autophagic protection against cisplatin-induced tissue injury in the kidney. *Genet Mol Res*. 2015;14(4):12006–15.
30. Hawley SA, Ford RJ, Smith BK, et al. The Na⁺/glucose cotransporter inhibitor canagliflozin activates AMPK by inhibiting mitochondrial function and increasing cellular AMP levels. *Diabetes*. 2016;65(9):2784–94.
31. Xie Z, Klionsky DJ. Autophagosome formation: core machinery and adaptations. *Nat Cell Biol*. 2007;9(10):1102–9.
32. Chen YC, Jandeleit-Dahm K, Peter K. Sodium-glucose cotransporter 2 (SGLT2) inhibitor dapagliflozin stabilizes diabetes-induced atherosclerotic plaque instability. *J Am Heart Assoc*. 2022;11(1):e022761.
33. Terasaki M, Hiromura M, Mori Y, et al. Amelioration of hyperglycemia with a sodium-glucose cotransporter 2 inhibitor prevents macrophage-driven atherosclerosis through macrophage foam cell formation suppression in type 1 and type 2 diabetic mice. *PLoS ONE*. 2015;10(11):e0143396.
34. Al-Sharea A, Murphy AJ, Huggins LA, Hu Y, Goldberg IJ, Nagareddy PR. SGLT2 inhibition reduces atherosclerosis by enhancing lipoprotein clearance in Ldlr(-/-) type 1 diabetic mice. *Atherosclerosis*. 2018;271:166–76.
35. Nasiri-Ansari N, Dimitriadis GK, Agrogiannis G, et al. Canagliflozin attenuates the progression of atherosclerosis and inflammation process in APOE knockout mice. *Cardiovasc Diabetol*. 2018;17(1):106.
36. Mori K, Tsuchiya K, Nakamura S, et al. Ipragliflozin-induced adipose expansion inhibits cuff-induced vascular remodeling in mice. *Cardiovasc Diabetol*. 2019;18(1):83.
37. Seneviratne A, Hulsmans M, Holvoet P, Monaco C. Biomechanical factors and macrophages in plaque stability. *Cardiovasc Res*. 2013;99(2):284–93.

Publisher's Note Springer Nature remains neutral with regard to jurisdictional claims in published maps and institutional affiliations.

Springer Nature or its licensor (e.g. a society or other partner) holds exclusive rights to this article under a publishing agreement with the author(s) or other rightsholder(s); author self-archiving of the accepted manuscript version of this article is solely governed by the terms of such publishing agreement and applicable law.